KSCE Journal of Civil Engineering (2019) 23(5):2303-2312

DOI 10.1007/s12205-019-1387-1

Structural Engineering

pISSN 1226-7988, eISSN 1976-3808
www.springer.com/12205

Nonlinear Vibration of a Stiffened Plate Considering the Existence of Initial Stresses

Tian-Qi Wang*, Rong-Hui Wang, and Niu-Jing Ma*****

Received July 18, 2018/Revised 1st: December 7, 2018, 2nd: January 22, 2019/Accepted January 23, 2019/Published Online March 4, 2019

Abstract

This paper presents a study on the nonlinear dynamic behavior of a stiffened plate with the existence of initial stresses. A stiffened plate is assumed to be composed of a plate and some stiffeners, which are treated separately. The plate is analyzed based on Thin Plate Theory, while the stiffeners are considered as geometrically nonlinear Euler-Bernoulli beams. The equations of both kinetic energies and strain energies of the plate and stiffeners are established. After that, the dynamic equilibrium equations for the stiffened plate are derived according to Lagrange equation. The nonlinear frequency for single-mode result is obtained through Elliptic function, and the accuracy of the analytical solution is verified through comparison with Ansys finite element method. In addition, homotopy analysis method is used to solve 3:1 internal resonance of the stiffened plate. With parametric analysis being conducted, the investigation on how initial stresses influence the nonlinear dynamic properties is carried out. Some useful nonlinear dynamic properties and conclusions are obtained, and thees can provide references for engineering application.

Keywords: *stiffened plates, initial stresses, nonlinear vibration, frequency, internal resonance*

1. Introduction

Stiffened plates are extensively used in engineering structures such as orthotropic steel bridge decks and fuselages of aircrafts. As is known to all, these types of structures are mainly subjected to dynamic loads, so the investigation on their dynamic behavior has become increasingly important in recent years.

For the past few years, increasing studies have been reported on the dynamic properties of stiffened plates. Sheikh and Mukhopadhyay (2002) utilized the spline finite strip method to both linear and nonlinear transient dynamic study of a stiffened plate. Peng *et al.* (2006) proposed a mesh-free Galerkin approach to analyze the dynamics of stiffened plates through the first-order shear deformable theory. Sapountzakis and Mokos (2008) proposed a general solution to the dynamic study of stiffened plates with parallel stiffeners placed arbitrarily in double symmetric cross-section. Gabor (2009) applied the new beam element with seven DOFs per node in analyzing the frequency and mode shape of each stiffened plate. Dozio and Ricciardi (2009) presented an efficient and easy-to-code approach for quickly predicting the modal characteristics of rectangular stiffened plates. Xu *et al.* (2010) came up with an analytical approach for the dynamic study of stiffened plates with stiffeners placed arbitrarily. Both the plate and stiffeners were simulated as 3-D components. Anirban *et al.* (2013) investigated the nonlinear dynamics of a stiffened plate by a variational method, and analyzed how stiffener position, plate aspect ratio, and stiffener-to-plate thickness ratio influenced the nonlinear vibrational properties. Ma *et al.* (2012, 2015) investigated the nonlinear vibration of stiffened plates under different resonance conditions based on Lagrange Equation. Parametric study was conducted and some significant nonlinear properties of stiffened plates were acquired. Duc *et al.* (2016) studied the nonlinear dynamics of shear deformable stiffened sandwich plates with imperfection on elastic foundation using the first-order shear deformation plate theory. Yuan and Jiang (2017) investigated the dynamic characteristics of stiffened multi-plates, with the displacement fields modeled by the first-order shear deformable plate and the Timoshenko beam theories. Yin *et al.* (2017) employed dynamic stiffness approach to investigate the dynamic transmission of built-up plate structures.

It is well known that the existence of initial stresses may have significant influence on structural mechanic behavior especially in dynamic analysis. Some researchers were dedicated to the study of initial stresses and obtained some achievements. Zheng and Hu (2005) studied the shake down effect of residual stresses in the rectangular plates on the stiffened panels and developed

*Ph.D. Candidate, School of Civil Engineering and Transportation, South China University of Technology, Guangzhou 510640, China (E-mail: 308578726@qq.com)
**Professor, School of Civil Engineering and Transportation, South China University of Technology, Guangzhou 510640, China; State Key Laboratory of Subtropical Building Science, Guangzhou 510640, China (E-mail: rhwang@scut.edu.cn)
***Associate Professor, School of Civil Engineering and Transportation, South China University of Technology, Guangzhou 510640, China; State Key Laboratory of Subtropical Building Science, Guangzhou 510640, China (Corresponding Author, E-mail: maniujing@yahoo.com)

the formula to calculate the level of shake down effect. Yuriy and Marina (2006) investigated the low-velocity impact on a prestressed circular orthotropic plate. Chen *et al.* (2007) studied the nonlinear properties of a laminated plate in a non-uniform initially stressed state. Numerical analysis manifested that initially stressed state had a remarkable effect on the dynamic properties of a laminate plate under nonlinear vibration. Owning to the wide application of stiffened plates in structural engineering field, it is essential to investigate how initial stresses influence the dynamic behavior of stiffened plates.

Homotopy analysis method is a type of universal analytical technique for both weakly and strongly nonlinear problems presented by Liao (2003) who systematically dealt with homotopy analysis method in his monograph, involving its basic concepts, principle together with its difference and relationship to other methods. Hoseini *et al.* (2008) derived a precise analytic solution for the nonlinear dynamics of a conservative oscillator via homotopy analysis method, showing this technique was effective for parametric analysis. Pirbodaghi *et al.* (2009) adopted homotopy analysis method to analyze the nonlinear dynamics of Euler-Bernoulli beams under axial loads. Through comparison with other commonly used methods, it demonstrated this method was highly accurate and effective for a variety of vibration amplitudes as well. Hassan and El-Tawil (2012) proposed to solve second-order nonlinear differential equations via homotopy analysis method. The results demonstrated accuracy and validity of the developed technique. Since it differs from perturbation approaches, homotopy analysis method is totally irrelevant to small parameters, thus it is suitable for most nonlinear problems. In addition to this, it also offers an easy means to guarantee the convergence of solution, so as to obtain precisely enough analytical approximations.

The purpose of this paper is to study a stiffened plate with initial stresses, which is different from the traditional study. Consider the initial stresses exist in the plate and stiffeners, respectively, and then energy principle and Lagrange's Equation are utilized to derive the nonlinear dynamic differential equations. Elliptic function method is used to solve the nonlinear frequency of the stiffened plate. The accuracy of the analytical solution is verified through comparison with Ansys finite element method. Additionally, homotopy analysis method is employed to investigate the 3:1 internal resonance upon considering primary resonance. Numerical analysis is performed to acquire some nonlinear dynamic properties, which are of great importance for engineering application.

2. Derivation of the Governing Equation

Figure 1 shows the structural diagram of a stiffened plate in which the displacements of the middle surface of the plate along x and y directions are represented by u and v, respectively, while w represents the displacement of the plate along z-direction. This stiffened plate is comprised of a plate as well as some uniformly spaced x-stiffeners and y-stiffeners. Both the plate and stiffeners use the same isotropic material. In the following, the plate and

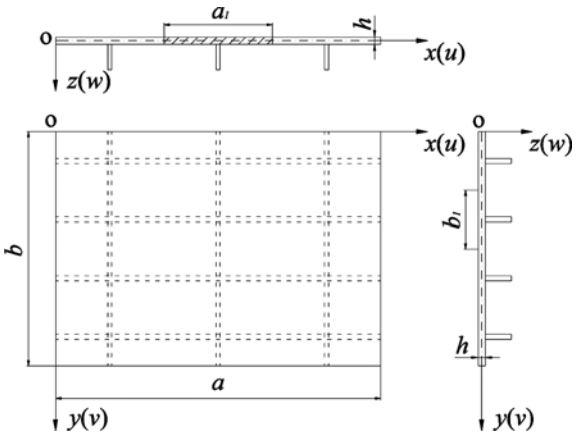

Fig. 1. Structure of a Stiffened Plate

stiffeners are treated separately, with the plate analyzed based on Thin Plate Theory, while Euler-Bernoulli Beam Theory used for stiffeners. In addition, the stresses and strains are given so as to formulate the strain energy equations of the plate and stiffeners, respectively. Then combining their kinetic energies, the nonlinear dynamic differential equations can be derived using Lagrange's Equation.

Since the actual initial stress distributions in engineering structures may be very complicated, they are usually simplified so as to be convenient for analysis. In this paper, the initial stresses are assumed to be σ_{px0} along x-direction and σ_{py0} along y-direction in the plate, and σ_{sx0} in x-stiffeners and σ_{sy0} in y-stiffeners. To simplify this study, all these initial stresses are assumed to be constant. In addition, self-equilibrium conditions for sectional stresses should be satisfied as:

$$\sigma_{px0} bh + \sigma_{sx0} A_{sx} N_{sx} = 0 \tag{1-1}$$

$$\sigma_{py0} ah + \sigma_{sy0} A_{sy} N_{sy} = 0 \tag{1-2}$$

where A_{sx} and A_{sy} are the sectional areas of x-stiffeners and y-stiffeners, respectively; N_{sx} and N_{sy} denote the numbers of x-stiffeners and y-stiffeners, respectively.

Based on Hooke's law, the relationships between stresses and strains for the plate and stiffeners are as follows:

$$\sigma_{pxx} = \frac{E}{1-\mu^2}\left(\varepsilon_{pxx} + \mu\varepsilon_{pyy}\right) \tag{2-1}$$

$$\sigma_{pyy} = \frac{E}{1-\mu^2}\left(\varepsilon_{pyy} + \mu\varepsilon_{pxx}\right) \tag{2-2}$$

$$\tau_{pxy} = \frac{E}{2(1+\mu)}\gamma_{pxy} \tag{2-3}$$

$$\sigma_{sx} = E\varepsilon_{sx} \tag{2-4}$$

$$\sigma_{sy} = E\varepsilon_{sy} \tag{2-5}$$

where σ_{pxx} and σ_{pyy} denote normal stresses in the plate relative to x and y directions, respectively; τ_{pxy} denotes shear stress of the plate relative to x and y directions; σ_{sx} and σ_{sy} denote normal stresses in x-stiffeners and y-stiffeners, respectively; ε_{pxx} and ε_{pyy} denote normal strains in the plate relative to x and y directions, respectively; γ_{pxy} denotes shear stress of the plate relative to x and y directions;

ε_{sx} and ε_{sy} denote normal stresses in *x*-stiffeners and *y*-stiffeners, respectively; and E and μ are Young's modulus and Poisson ratio of the material of stiffened plates, respectively.

On the basis of Eqs. (2-1) to (2-5), the initial strains in the plate and stiffeners can be given by:

$$\varepsilon_{px0}=\frac{1}{E}\left(\sigma_{px0}-\mu\sigma_{py0}\right) \tag{3-1}$$

$$\varepsilon_{py0}=\frac{1}{E}\left(\sigma_{py0}-\mu\sigma_{px0}\right) \tag{3-2}$$

$$\varepsilon_{sx0}=\frac{\sigma_{sx0}}{E} \tag{3-3}$$

$$\varepsilon_{sy0}=\frac{\sigma_{sy0}}{E} \tag{3-4}$$

Upon considering the geometric nonlinearity of the plate and stiffeners and combing Eqs. (3-1) to (3-4), the strains of the plate and stiffeners can be given by:

$$\varepsilon_{pxx}=\frac{\partial u}{\partial x}+\frac{1}{2}\left(\frac{\partial w}{\partial x}\right)^2-z\frac{\partial^2 w}{\partial x^2}+\frac{1}{E}\left(\sigma_{px0}-\mu\sigma_{py0}\right) \tag{4-1}$$

$$\varepsilon_{pyy}=\frac{\partial v}{\partial y}+\frac{1}{2}\left(\frac{\partial w}{\partial y}\right)^2-z\frac{\partial^2 w}{\partial y^2}+\frac{1}{E}\left(\sigma_{py0}-\mu\sigma_{px0}\right) \tag{4-2}$$

$$\gamma_{pxy}=\frac{\partial u}{\partial y}+\frac{\partial v}{\partial x}+\frac{\partial w}{\partial x}\frac{\partial w}{\partial y}-2z\frac{\partial^2 w}{\partial x\partial y} \tag{4-3}$$

$$\varepsilon_{sx}=\frac{\partial u}{\partial x}+\frac{1}{2}\left(\frac{\partial w}{\partial x}\right)^2-z\frac{\partial^2 w}{\partial x^2}+\frac{\sigma_{sx0}}{E} \tag{4-4}$$

$$\varepsilon_{sy}=\frac{\partial v}{\partial y}+\frac{1}{2}\left(\frac{\partial w}{\partial y}\right)^2-z\frac{\partial^2 w}{\partial y^2}+\frac{\sigma_{sy0}}{E} \tag{4-5}$$

The strain energy of the plate is given by:

$$U_p=\frac{1}{2}\int_{\Omega_p}\left(\sigma_{pxx}\varepsilon_{pxx}+\sigma_{pyy}\varepsilon_{pyy}+\tau_{pxy}\gamma_{pxy}\right)\mathrm{d}V \tag{5}$$

The stresses and strains of the plate can refer to Eqs. (2-1) to (2-3) and Eqs. (4-1) to (4-3).

Similarly, the strain energies of x-stiffeners and y-stiffeners are given by:

$$U_{sx}=\frac{1}{2}\int_{\Omega_{sx}}\sigma_{sx}\varepsilon_{sx}\mathrm{d}V \tag{6-1}$$

$$U_{sy}=\frac{1}{2}\int_{\Omega_{sy}}\sigma_{sy}\varepsilon_{sy}\mathrm{d}V \tag{6-2}$$

The kinetic energy of the plate is:

$$T_p=\frac{1}{2}\rho h\int_0^a\int_0^b\left[\left(\frac{\partial u}{\partial t}\right)^2+\left(\frac{\partial v}{\partial t}\right)^2+\left(\frac{\partial w}{\partial t}\right)^2\right]\mathrm{d}x\mathrm{d}y \tag{7}$$

where ρ is the mass per unit volume of the material, while h is the thickness of the plate.

For stiffeners, the kinetic energy of the *i*th *x*-stiffener and *y*-stiffener is given as follows:

$$T_{sxi}=\frac{1}{2}\rho A_x\int_0^a\left[\left(\frac{\partial u}{\partial t}\right)^2+\left(\frac{\partial v}{\partial t}\right)^2+\left(\frac{\partial w}{\partial t}\right)^2\right]\mathrm{d}x\Bigg|_{y=y_i}\qquad i=1,\cdots,N_{sx} \tag{8-1}$$

$$T_{syi}=\frac{1}{2}\rho A_y\int_0^b\left[\left(\frac{\partial u}{\partial t}\right)^2+\left(\frac{\partial v}{\partial t}\right)^2+\left(\frac{\partial w}{\partial t}\right)^2\right]\mathrm{d}y\Bigg|_{x=x_i}\qquad i=1,\cdots,N_{sy} \tag{8-2}$$

where the coordinates of *i*th *x*-stiffener and *y*-stiffener are $y=y_i$ and $x=x_i$, respectively.

The total strain energy U of the stiffened plate can be expressed as:

$$U=U_p+U_{sx}+U_{sy} \tag{9}$$

The total kinetic energy T of the stiffened plate can be expressed as:

$$T=T_p+\sum_{i=1}^{N_{sx}}T_{sxi}+\sum_{i=1}^{N_{sy}}T_{syi} \tag{10}$$

For a stiffened plate investigated in this paper, it is considered to be subjected to transverse excitation, which acts along *z*-direction, and it is expressed as:

$$q(x,y,t)=F\cos(\Omega t) \tag{11}$$

where F is the amplitude of the transverse excitation; and Ω is the frequency of the transverse excitation.

The displacements of the stiffened plate are assumed to be the product of time function and space function, and then they are expressed in terms of tensors as follows:

$$u(x,y,t)=u_{ij}^t(t)u_{ij}^d(x,y)\quad i=1,\cdots,\bar{M};j=1,\cdots,\bar{N} \tag{12-1}$$

$$v(x,y,t)=v_{ij}^t(t)v_{ij}^d(x,y)\quad i=1,\cdots,\bar{M};j=1,\cdots,\bar{N} \tag{12-2}$$

$$w(x,y,t)=w_{ij}^t(t)w_{ij}^d(x,y)\quad i=1,\cdots,M;i=1,\cdots,N \tag{12-3}$$

where $u_{ij}^t(t)$, $v_{ij}^t(t)$ and $w_{ij}^t(t)$ are the generalized coordinates along *x*, *y* and *z* directions, respectively; $u_{ij}^d(x,y)$, $v_{ij}^d(x,y)$ and $w_{ij}^d(x,y)$ are the mode functions along *x*, *y* and *z* directions, respectively; $\bar{M}$ and $\bar{N}$ denote the necessary terms of the in-plane expansion displacements; and M and N denote the necessary terms of the out-of-plane expansion displacements.

Combining Eqs. (9) to (12) and using Lagrange's Equation, the following formulation can be obtained:

$$\frac{\mathrm{d}^2\left(u_{mn}^t\right)}{\mathrm{d}t^2}g_{ijmn}^1+c_{ij}^1+u_{mn}^t d_{ijmn}^1+v_{mn}^t d_{ijmn}^2+w_{mn}^t d_{ijmn}^3+w_{mn}^t w_{kl}^t e_{ijmnkl}^1=Q_{u_{ij}} \tag{13-1}$$

$$\frac{\mathrm{d}^2\left(v_{mn}^t\right)}{\mathrm{d}t^2}g_{ijmn}^2+c_{ij}^2+u_{mn}^t d_{ijmn}^4+v_{mn}^t d_{ijmn}^5+w_{mn}^t d_{ijmn}^6+w_{mn}^t w_{kl}^t e_{ijmnkl}^2=Q_{v_{ij}} \tag{13-2}$$

$$\begin{aligned}&\frac{\mathrm{d}^2\left(w_{mn}^t\right)}{\mathrm{d}t^2}g_{ijmn}^3+c_{ij}^3+u_{mn}^t d_{ijmn}^7+v_{mn}^t d_{ijmn}^8+w_{mn}^t d_{ijmn}^9\\&+u_{mn}^t w_{kl}^t e_{ijmnkl}^3+v_{mn}^t w_{kl}^t e_{ijmnkl}^4+w_{mn}^t w_{kl}^t e_{ijmnkl}^5+w_{mn}^t w_{kl}^t w_{pq}^t f_{ijmnklpq}=Q_{w_{ij}}\end{aligned} \tag{13-3}$$

In Eqs. (13-1) to (13-3), the specific expression of each coefficient tensor is listed in Appendix A, while Q_{uij}, Q_{vij} and Q_{wij} are the generalized forces regarding generalized coordinates u_{ij}^t, v_{ij}^t and w_{ij}^t, respectively. The generalized forces can be expressed as:

$$Q=\frac{\delta W}{\delta q} \tag{14}$$

where W is the virtual work with respect to the generalized

coordinate q like aforementioned u_{ij}^{l}, v_{ij}^{l} and w_{ij}^{l}.

The in-plane inertia terms are neglected here, since their effect is usually far less than that of the transverse inertia term (Amabili, 2008; Noseir and Reddy, 1991; Chia, 1980). Meanwhile, dimensionless formulation is introduced by putting:

$$u_{ij}^{*}=au_{ij}^{l}/h^{2},\quad v_{ij}^{*}=bv_{ij}^{l}/h^{2},\quad w_{ij}^{*}=w_{ij}^{l}/h,\quad \tau=t\sqrt{\frac{E}{\rho h^{2}}} \tag{15}$$

Then, Eqs. (12-1)–(12-3) can be written in dimensionless forms as:

$$c_{ij}^{1*}+u_{mn}^{*}d_{ijmn}^{1*}+v_{mn}^{*}d_{ijmn}^{2*}+w_{mn}^{*}d_{ijmn}^{3*}+w_{mn}^{*}w_{kl}^{*}e_{ijmnkl}^{1*}=Q_{u_{ij}} \tag{16-1}$$

$$c_{ij}^{2*}+u_{mn}^{*}d_{ijmn}^{4*}+v_{mn}^{*}d_{ijmn}^{5*}+w_{mn}^{*}d_{ijmn}^{6*}+w_{mn}^{*}w_{kl}^{*}e_{ijmnkl}^{2*}=Q_{v_{ij}} \tag{16-2}$$

$$\begin{aligned}&\frac{\mathrm{d}^{2}\left(w_{mn}^{*}\right)}{\mathrm{d}\tau^{2}}g_{ijmn}^{3*}+c_{ij}^{3*}+u_{mn}^{*}d_{ijmn}^{7*}+v_{mn}^{*}d_{ijmn}^{8*}+w_{mn}^{*}d_{ijmn}^{9*}\\&+u_{mn}^{*}w_{kl}^{*}e_{ijmnkl}^{3*}+v_{mn}^{*}w_{kl}^{*}e_{ijmnkl}^{4*}\\&+w_{mn}^{*}w_{kl}^{*}e_{ijmnkl}^{5*}+w_{mn}^{*}w_{kl}^{*}w_{pq}^{*}f_{ijmnklpq}^{*}=Q_{w_{ij}}\end{aligned} \tag{16-3}$$

In Eqs. (16-1) to (16-3), the specific expression of each coefficient tensor is related to that in Eqs. (13-1) to (13-3), and not listed here.

3. Numerical Analysis

3.1 Nonlinear Frequency Analysis

3.1.1 Methodology

It is significant to investigate the fundamental frequency for engineering structures since the first mode usually plays a dominant role in vibration. In this paper, the four edges clamped condition is selected for analysis in the following work, and the displacements are given as follows:

$$u(x,y,t)=\sum_{m=1}^{\bar{M}}\sum_{n=1}^{\bar{N}}u_{mn}^{l}(t)\sin\frac{2m\pi(x-a/2)}{a}\cos\frac{(2n-1)\pi(y-b/2)}{b} \tag{17-1}$$

$$v(x,y,t)=\sum_{m=1}^{\bar{M}}\sum_{n=1}^{\bar{N}}v_{mn}^{l}(t)\cos\frac{(2m-1)\pi(x-a/2)}{a}\sin\frac{2n\pi(y-b/2)}{b} \tag{17-2}$$

$$w(x,y,t)=\sum_{m=1}^{\bar{M}}\sum_{n=1}^{\bar{N}}w_{mn}^{l}(t)\left[\cos\frac{2m\pi(x-a/2)}{a}-(-1)^{m}\right]\left[\cos\frac{2n\pi(y-b/2)}{b}-(-1)^{n}\right] \tag{17-3}$$

For the $(1,1)^{st}$ mode, choosing the first terms in Eqs. (17-1)–(17-3) and writing them in dimensionless forms, substituting them into Eqs. (16-1)–(16-3) and letting the generalized forces Q_{uij}, Q_{vij} and Q_{wij} equal 0, then the following nonlinear dynamic differential equation can be obtained as:

$$\frac{\mathrm{d}^{2}}{\mathrm{d}\tau^{2}}\left(w_{11}^{*}\right)+\alpha w_{11}^{*}+\beta\left(w_{11}^{*}\right)^{3}=0 \tag{18}$$

where

$$\alpha=\frac{\left(\frac{d_{1111}^{3*}d_{1111}^{5*}}{d_{1111}^{2*}}-d_{1111}^{6*}\right)d_{1111}^{7*}}{d_{1111}^{4*}-\frac{d_{1111}^{1*}d_{1111}^{5*}}{d_{1111}^{2*}}}+\frac{\left(\frac{d_{1111}^{3*}d_{1111}^{4*}}{d_{1111}^{1*}}-d_{1111}^{6*}\right)d_{1111}^{8*}}{d_{1111}^{5*}-\frac{d_{1111}^{2*}d_{1111}^{4*}}{d_{1111}^{1*}}}+d_{1111}^{9*} \tag{19-1}$$

$$\beta=f_{11111111}^{*} \tag{19-2}$$

3.1.2 Numerical Analysis

The parameters of a stiffened plate (made of steel) studied in this paper are listed as follows: $a=1.5$ m, $b=1$ m, $E=2.0\times10^{11}$ Pa, $m=0.3$, $r=7.85\times10^{3}$ kg/m^{3}, $h=0.01$ m, the height of each stiffener is 0.1 m, and the width of each stiffener is 0.02 m. The initial stresses are considered as Case 1: $\sigma_{px0}=\sigma_{py0}=-20$ Mpa, Case 2: $\sigma_{px0}=\sigma_{py0}=-10$ MPa, Case 3: $\sigma_{px0}=\sigma_{py0}=0$, Case 4: $\sigma_{px0}=\sigma_{py0}=10$ MPa, Case 5: $\sigma_{px0}=\sigma_{py0}=20$ MPa. In addition, 6 types of stiffened plates with different stiffener configuration are investigated for comparison including: 1) one stiffener along both x and y directions ($N_{sx}=N_{sy}=1$); 2) three stiffeners along both the two directions ($N_{sx}=N_{sy}=3$); 3) five stiffeners along both the two directions ($N_{sx}=N_{sy}=5$); 4) one stiffener along only x direction ($N_{sx}=1$); 5) three stiffeners along only x direction ($N_{sx}=3$); and 6) five stiffeners along only x direction ($N_{sx}=5$). Figs. 2–7 show the relationship between nonlinear frequency ratio and its amplitude of the stiffened plates, where the nonlinear frequency ratio f is represented by the ratio of the nonlinear frequency to linear frequency, while the amplitude A_c is denoted by the ratio of the amplitude of plate center to plate thickness.

To illustrate the accuracy, the results of the analytical solution are compared with those of the finite element analysis via Ansys. For simplification, the following analysis only considers Case 1

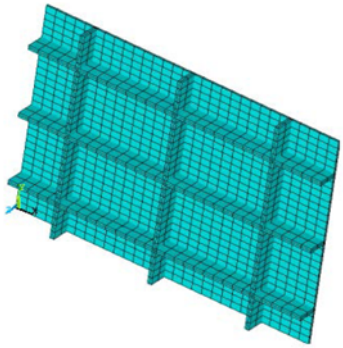

Fig. 2. Ansys Finite Element Mode

Table 1. Nonlinear Frequency Analysis

Amplitude A	Nonlinear frequency ratio f	
	Present results	Ansys results
0	1.000	1.000
0.1	1.001	1.001
0.2	1.005	1.005
0.3	1.012	1.011
0.4	1.021	1.020
0.5	1.032	1.030
0.6	1.046	1.043
0.7	1.062	1.058
0.8	1.081	1.077
0.9	1.101	1.095
1.0	1.124	1.116

and $N_{sx} = N_{sy} = 3$. The plate is modeled by Shell181 element, while the stiffeners are modeled by Beam188 element. The size of both Shell181 and Beam4 elements is 5 cm along x direction and 10/3 cm along y direction. The boundary conditions are four edges clamped. Fig. 2 is the Ansys finite element model.

The nonlinear frequency ratio f is listed in Table 1.

From Table 1, it can be observed the present results agree well with Ansys results, especially in low-amplitude vibration. Besides, the present values are less than those from Ansys, and this can be explained by the difference of interpolation functions between the two methods. The aforementioned analysis also shows the first mode plays a dominant role in vibration.

According to Figs. 3–8, it can be observed that nonlinear frequency ratio increases with the rise of amplitude, and it also increases from Case 1 to Case 5, consequently, it is obvious that the nonlinear frequency ratio of a stiffened plate increases from the compressed status of the plate to its tensile status. This also means the nonlinear frequency ratio of a stiffened plate decreases from the compressed status of the stiffeners to their tensile status. Then this phenomenon can be explained by the fact that the bending stiffness of stiffeners usually plays a dominant role in a stiffened plate, and it will become larger and increase when the tensile stress in the stiffeners arises and continue rising with the plate under compressed status, as a result, the nonlinear behavior of the stiffened plate becomes weaker, and vice versa.

Comparing Figs. 3–5 with Figs. 6–8, a stiffened plate with stiffeners in both directions can decrease the nonlinear behavior even more remarkably than that with stiffeners in only one direction. This means it is better to set stiffeners in two directions than in only one direction.

Additionally, as can be seen from Figs. 3–5, the nonlinear frequency ratio varies slightly between 3 stiffeners and 5 stiffeners

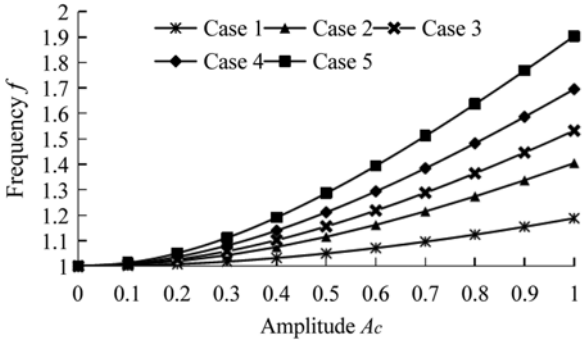

Fig. 3. Nonlinear Frequencies of the Stiffened Plate when $N_{sx} = N_{sy} = 1$

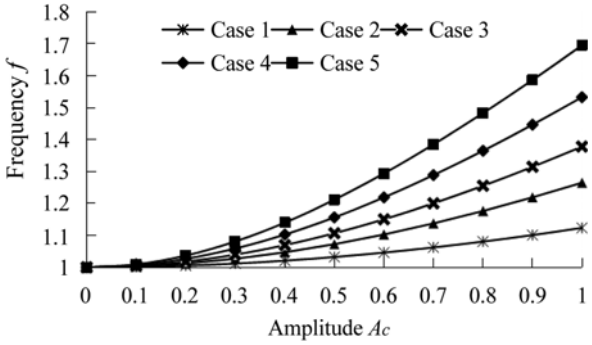

Fig. 4. Nonlinear Frequencies of the Stiffened Plate when $N_{sx} = N_{sy} = 3$

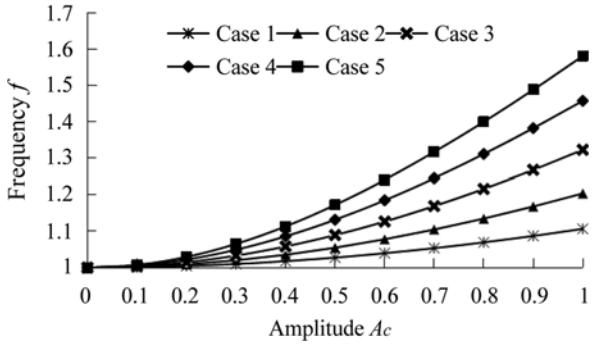

Fig. 5. Nonlinear Frequencies of the Stiffened Plate when $N_{sx} = N_{sy} = 5$

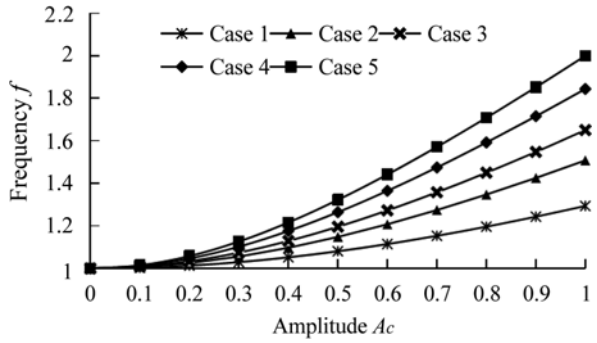

Fig. 6.Nonlinear Frequencies of the Stiffened Plate when $N_{sx} = 1$

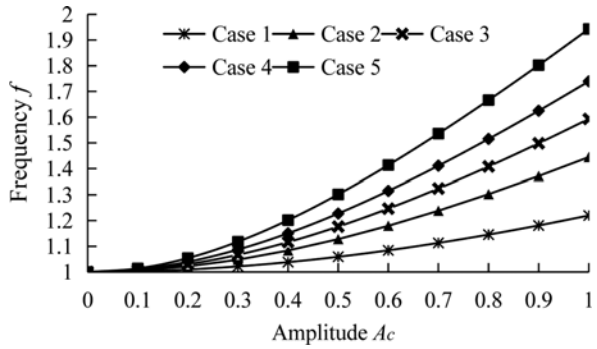

Fig. 7. Nonlinear Frequencies of the Stiffened Plate when $N_{sx} = 3$

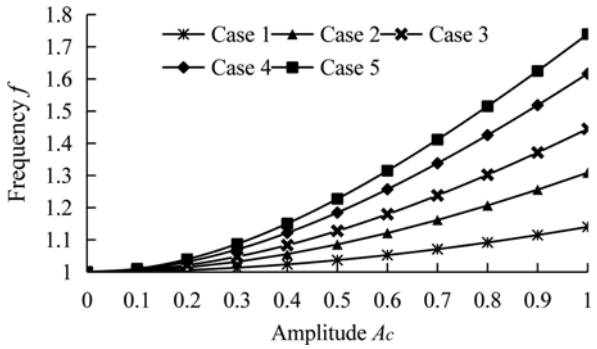

Fig. 8. Nonlinear Frequencies of the Stiffened Plate when $N_{sx} = 5$

in two directions, which demonstrates the nonlinear behavior of a stiffened plate is affected less obviously by stiffeners after the number of stiffeners in both direction exceeds 3.

3.2 Internal Resonance Analysis

3.2.1 Methodology

For a nonlinear dynamic differential equation with cubic terms, the internal resonance may occur when the rate of the natural frequencies between two modes is close to 3:1. Take aforementioned boundary condition into consideration and the displacements of the stiffened plate for double-mode transverse vibration are given as follows:

$$u(x,y,t)=u_{11}^{I}(t)\sin\frac{2\pi(x-a/2)}{a}\cos\frac{\pi(y-b/2)}{b} \tag{20-1}$$

$$v(x,y,t)=v_{11}^{I}(t)\cos\frac{\pi(x-a/2)}{a}\sin\frac{2\pi(y-b/2)}{b} \tag{20-2}$$

$$w(x,y,t)=w_{11}^{I}(t)\left[\cos\frac{2\pi(x-a/2)}{a}+1\right]\left[\cos\frac{2\pi(y-b/2)}{b}+1\right]$$
$$+w_{13}^{I}(t)\left[\cos\frac{2\pi(x-a/2)}{a}+1\right]\left[\cos\frac{6\pi(y-b/2)}{b}+1\right] \tag{20-3}$$

Writing Eqs. (20-1)–(20-3) in dimensionless forms and using Eqs. (16-1)–(16-3), the nonlinear dynamic differential equations of the stiffened plate are obtained as:

$$\ddot{w}_{11}^{*}+p_{1,1}w_{11}^{*}+p_{1,2}\left(w_{13}^{*}\right)^{3}+p_{1,3}w_{11}^{*}\left(w_{13}^{*}\right)^{2}$$
$$+p_{1,4}\left(w_{11}^{*}\right)^{2}w_{13}^{*}+p_{1,5}\left(w_{11}^{*}\right)^{3}=p_{1,6}\cos\left(\Omega^{*}\tau\right) \tag{21-1}$$

$$\ddot{w}_{13}^{*}+p_{3,1}w_{13}^{*}+p_{3,2}\left(w_{13}^{*}\right)^{3}+p_{3,3}w_{11}^{*}\left(w_{13}^{*}\right)^{2}$$
$$+p_{3,4}\left(w_{11}^{*}\right)^{2}w_{13}^{*}+p_{3,5}\left(w_{11}^{*}\right)^{3}=p_{3,6}\cos\left(\Omega^{*}\tau\right) \tag{21-2}$$

where the non-dimensional frequency of the transverse excitation $\Omega^{*}=\Omega\sqrt{\frac{\rho h^{2}}{E}}$; and the expressions of $p_{1,1}$–$p_{1,6}$ and $p_{3,1}$–$p_{3,6}$ are related to coefficient tensors.

In the following work, 3:1 internal resonance between the $(1,1)^{st}$ and $(1,3)^{rd}$ modes are investigated using homotopy analysis method put forth by Liao (2003). Here, primary resonance is also dealt with by considering the excitation frequency approaching the fundamental frequency. In order to investigate internal these two types of resonance cases, two detuning parameters σ_1 and σ_2 should be introduced, and assume:

$$\omega_{3}^{*}=3\omega_{1}^{*}+\sigma_{1} \tag{22-1}$$

$$\Omega^{*}=\omega_{1}^{*}+\sigma_{2} \tag{22-2}$$

In Eqs. (22-1) and (22-2), $w_{1n}^{*}(\tau)$ is expressed by $r_n(\tau)$, and then the periodic solution can be written as:

$$r_n(\tau)=\sum_{k=1}^{+\infty}\lambda_{n,k}\cos\left(kn\Omega^{*}\tau+\theta_n\right) \tag{23}$$

where $\lambda_{n,k}$ is an unknown real number; θ_n is a phase angle.

Prior to solving Eqs. (21-1) and (21-2), we define a nonlinear operator as:

$$r_n(\tau)=\sum_{k=1}^{+\infty}\lambda_{n,k}\cos\left(kn\Omega^{*}\tau+\theta_n\right) \tag{24}$$

where $\phi_n(\tau,s)$ is an unknown real number.

A zero*th*-order deformation equation is established as:

$$(1-s)L_n\left[\phi_n(\tau,s)-r_{n,0}(\tau)\right]=s\hbar H(\tau)N_n\left[\phi_1(\tau,s),\phi_3(\tau,s)\right] \tag{25}$$

where $s\in[0,1]$ is an embedding parameter; L_n is a auxiliary linear operator; $r_{n,0}(\tau)$ is an initial approximation of $r_n(\tau)$; $\hbar$ is a non-zero real number; and $H(\tau)$ is an auxiliary real function.

On the basis of Eq. (23), choose auxiliary linear operator as:

$$L_n\left[\phi_n(\tau,s)\right]=\frac{\partial^{2}\phi_n(\tau,s)}{\partial\tau^{2}}+\left(n\Omega^{*}\right)^{2}\phi_n(\tau,s) \tag{26}$$

The initial approximation $r_{n,0}(\tau)$ is given by:

$$r_{n,0}(\tau)=\lambda_{n,1}\cos\left(n\Omega^{*}\tau+\theta_n\right) \tag{27}$$

Expand $\phi_n(\tau,s)$ in terms of Taylor's series, and we get:

$$\phi_n(\tau,s)=r_{n,0}(\tau)+\sum_{k=1}^{+\infty}r_{n,k}(\tau)s^{k} \tag{28}$$

where

$$r_{n,k}(\tau)=\frac{1}{k!}\frac{\partial^{k}\phi_n(\tau,s)}{\partial s^{k}}\bigg|_{s=0} \tag{29}$$

If $\hbar$ and $H(\tau)$ are proper, the series will converge once $s=1$. Accordingly, the following can be obtained:

$$r_n(\tau)=r_{n,0}(\tau)+\sum_{k=1}^{+\infty}r_{n,k}(\tau) \tag{30}$$

Let Eq. (25) be differentiated for m times regarding to s and then let $s=0$. After that, this equation is divided by $k!$, leading to the following the k^{th}-order deformation as:

$$L_n\left[r_{n,k}(\tau)-\chi_{n,k}r_{n,k-1}(\tau)\right]=\hbar H(\tau)R_{n,k}(\tau) \tag{31}$$

where

$$R_{n,k}(\tau)=\frac{1}{(k-1)!}\frac{\partial^{k-1}N_n\left[\phi_1(\tau,s),\phi_3(\tau,s)\right]}{\partial s^{k-1}}\bigg|_{s=0} \tag{32-1}$$

$$\chi_{n,k}=\begin{cases}0, & k\le 1\\ 1, & k>1\end{cases} \tag{32-2}$$

To abide by the law of expressions of solutions and ergodicity of coefficients, the auxiliary real function can be defined as:

$$H(\tau)=1 \tag{33}$$

To investigate primary resonance of Eqs. (21-1)–(21-2), let $k=1$. On the basis of Eq. (32-1), the following can be obtained:

$$R_{1,1}(\tau)=\ddot{r}_{1,0}+\left(\omega_{1}^{*}\right)^{2}r_{1,0}+p_{1,2}\left(r_{3,0}\right)^{3}+p_{1,3}r_{1,0}\left(r_{3,0}\right)^{2}$$
$$+p_{1,4}\left(r_{1,0}\right)^{2}r_{3,0}+p_{1,5}\left(r_{1,0}\right)^{3}-p_{1,6}\cos\left(\Omega^{*}\tau\right) \tag{34-1}$$

$$R_{3,1}(\tau)=\ddot{r}_{3,0}+\left(\omega_3^*\right)^2 r_{3,0}+p_{3,2}\left(r_{3,0}\right)^3+p_{3,3}r_{1,0}\left(r_{3,0}\right)^2$$
$$+p_{3,4}\left(r_{1,0}\right)^2 r_{3,0}+p_{3,5}\left(r_{1,0}\right)^3-p_{3,6}\cos\left(\Omega^*\tau\right) \quad (34\text{-}2)$$

where $\left(\omega_n^*\right)^2=p_{n,1}$, ω_n^* is the n^{th}-order dimensionless natural frequency of the derived system.

Substituting Eq. (27) into Eqs. (34-1)–(34-2) and using the solvability condition of eliminating permanent terms yields:

$$-\frac{1}{2}\left(\omega_1^*+\sigma_2\right)^2\lambda_{1,1}\cos\theta_1+\frac{1}{2}\left(\omega_1^*\right)^2\lambda_{1,1}\cos\theta_1+\frac{1}{4}p_{1,3}\lambda_{1,1}\left(\lambda_{3,1}\right)^2\cos\theta_1$$
$$+\frac{1}{8}p_{1,4}\left(\lambda_{1,1}\right)^2\lambda_{3,1}\cos\left(-2\theta_1+\theta_3\right)+\frac{3}{8}p_{1,5}\left(\lambda_{1,1}\right)^3\cos\theta_1-\frac{1}{2}p_{1,6}=0 \quad (35\text{-}1)$$

$$-\frac{1}{2}\left(\omega_1^*+\sigma_2\right)^2\lambda_{1,1}\sin\theta_1+\frac{1}{2}\left(\omega_1^*\right)^2\lambda_{1,1}\sin\theta_1+\frac{1}{4}p_{1,3}\lambda_{1,1}\left(\lambda_{3,1}\right)^2\sin\theta_1$$
$$+\frac{1}{8}p_{1,4}\left(\lambda_{1,1}\right)^2\lambda_{3,1}\sin\left(-2\theta_1+\theta_3\right)+\frac{3}{8}p_{1,5}\left(\lambda_{1,1}\right)^3\sin\theta_1=0 \quad (35\text{-}2)$$

$$-\frac{9}{2}\left(\omega_1^*+\sigma_2\right)^2\lambda_{3,1}\cos\theta_3+\frac{1}{2}\left(3\omega_1^*+\sigma_1\right)^2\lambda_{3,1}\cos\theta_3+\frac{3}{8}p_{3,2}\left(\lambda_{3,1}\right)^3\cos\theta_3$$
$$+\frac{1}{4}p_{3,4}\left(\lambda_{1,1}\right)^2\lambda_{3,1}\cos\theta_3+\frac{1}{4}p_{3,5}\left(\lambda_{1,1}\right)^3\cos 3\theta_1=0 \quad (35\text{-}3)$$

$$-\frac{9}{2}\left(\omega_1^*+\sigma_2\right)^2\lambda_{3,1}\sin\theta_3+\frac{1}{2}\left(3\omega_1^*+\sigma_1\right)^2\lambda_{3,1}\sin\theta_3+\frac{3}{8}p_{3,2}\left(\lambda_{3,1}\right)^3\sin\theta_3$$
$$+\frac{1}{4}p_{3,4}\left(\lambda_{1,1}\right)^2\lambda_{3,1}\sin\theta_3+\frac{1}{4}p_{3,5}\left(\lambda_{1,1}\right)^3\sin 3\theta_1=0 \quad (35\text{-}4)$$

Equations (35-1)–(35-4) are four transcendental equations, therefore, the expressions of $\lambda_{1,1}$, $\lambda_{3,1}$, θ_1 and θ_3 are not likely to be got through them. Here, Newton-Raphson approach may be applied to get the nontrivial solutions $\lambda_{1,1}$, $\lambda_{3,1}$, θ_1 and θ_3.

According to Eqs. (27) and (35-1)–(35-4), the first approximate solutions of the double-modal system are obtained as:

$$r_{1,0}(\tau)=\lambda_{1,1}\cos\left(\Omega^*\tau+\theta_1\right) \quad (36\text{-}1)$$

$$r_{3,0}(\tau)=\lambda_{3,1}\cos\left(3\Omega^*\tau+\theta_3\right) \quad (36\text{-}2)$$

Similarly, the higher-order approximate solutions can be obtained according to Eq. (26). Due to space limitations, it is not dealt with in this paper.

3.2.1 Numerical Analysis

Consider the same parameters of the stiffened plate as Section 3.1. Besides, the amplitude of the transverse excitation F = 1 kN/m^2 and the frequency of excitation $\Omega^*=0.99\ \omega_1^*$. For simplification, the initial stresses are considered as Case 1: $\sigma_{px0}=\sigma_{py0}=-20$ Mpa, Case 2: $\sigma_{px0}=\sigma_{py0}=0$, Case 3: $\sigma_{px0}=\sigma_{py0}=20$ MPa. In the following analysis, we consider the internal resonance is completely detuned. Based on the aforementioned parameters, the time-history curves $r_{1,0}$-τ and $r_{3,0}$-τ as well as the amplitude-frequency curves $\lambda_{1,1}$-σ_2 and $\lambda_{1,3}$-σ_2 under primary resonance are plotted as shown in Figs. 9–13.

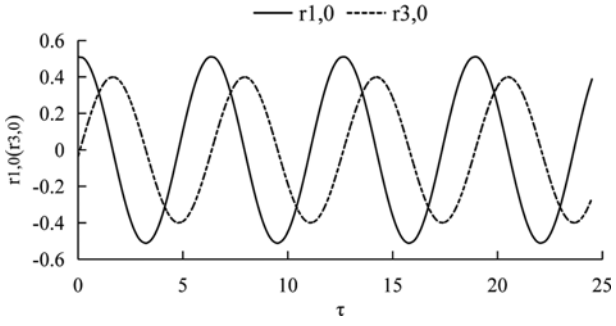

Fig. 9. Time-history Curves under Case 1

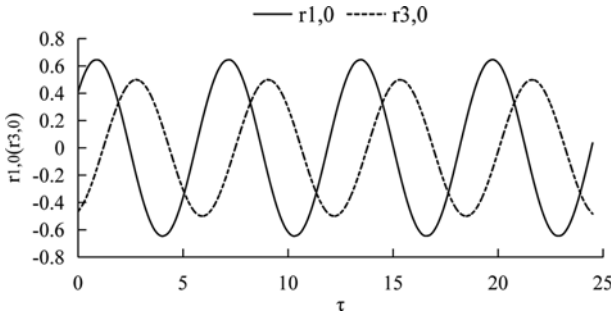

Fig. 10. Time-history Curves under Case 2

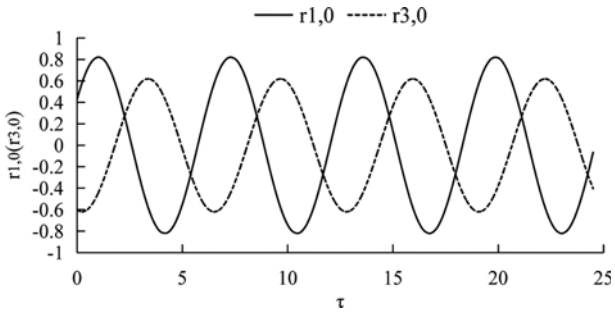

Fig. 11. Time-history Curves under Case 3

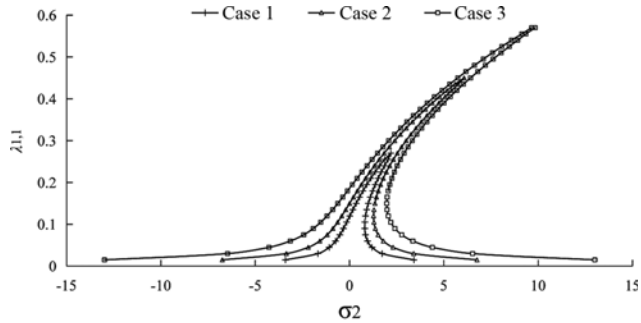

Fig. 12. Amplitude-Frequency Curves for $\lambda_{1,1}$-σ_2

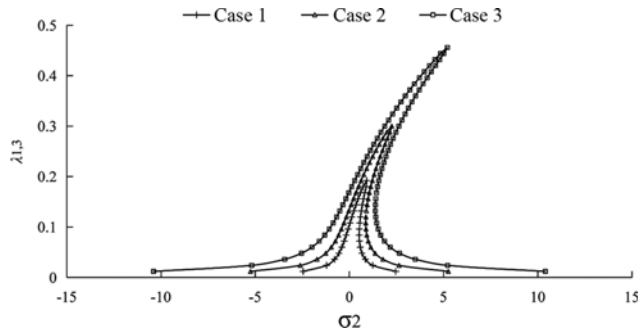

Fig. 13. Amplitude-Frequency Curves for $\lambda_{1,3}$-σ_2

From Figs. 9–13, it can be observed that both the two coupled modes are excited once the external excitation works. Since the $(1,1)^{st}$ mode is excited directly by the external excitation while the $(1,3)^{rd}$ mode is excited by the $(1,1)^{st}$ mode, the amplitude of the $(1,1)^{st}$ mode is larger than that of the $(1,3)^{rd}$ mode during the energy exchange. Meanwhile, the amplitude becomes larger gradually from Figs. 9–11. This can also be explained by the fact that the stiffeners experience the stages from tensile status to compressed status with the stress status of the plate changing, which decreases the total stiffness of the stiffened plate, thereby strengthening the nonlinear behavior of the stiffened plate.

4. Conclusions

This paper focuses on the nonlinear dynamic behavior of a stiffened plate with initial stresses. Energy principle and Lagrange's Equation are utilized to derive the nonlinear dynamic differential equations. Elliptic function method is used to solve the nonlinear frequency of the stiffened plate. The results in the paper match with those in Ansys, so the accuracy of the analytical solution can be verified. Additionally, homotopy analysis method is employed to investigate the 3:1 internal resonance upon considering primary resonance. Numerical analysis is performed and some important conclusions are drawn as follows:

1. Due to the fact that the bending stiffness of stiffeners usually plays a dominant role in a stiffened plate, and it increases with the tensile stress arising and increasing, the nonlinear behavior of the stiffened plate will become weaker, and vice versa.
2. A stiffened plate with stiffeners in double directions has more remarkable influence on the nonlinear behavior than that with stiffeners in only one direction.
3. As no small parameter is needed in homotopy analysis method, its application range is more extensive, and it can be applied to both weakly and strongly nonlinear problems.
4. In view of internal resonance functioning, the coupled mode can be excited simultaneously on account of the exchange of energy between two coupled modes, but its amplitude is smaller than that excited directly by the external excitation.
5. There are hard spring characteristic, jumping phenomena and multi-value property in the amplitude-frequency curve owing to the geometrical nonlinearity working. The geometrical nonlinearity has significant effects on the dynamic properties of stiffened plates, therefore it is essential to take the geometrical nonlinearity into consideration when studying the mechanical properties of this kind of structures.

Acknowledgements

The authors gratefully acknowledge the support of National Natural Science Foundation of China (No.51408228 and No.51478192) and State Key Lab of Subtropical Building Science, South China University of Technology (No.2018ZB31).

References

Amabili, M. (2008). *Nonlinear vibrations and stability of shells and plates*, Cambridge University Press, Cambridge, England.

Anirban, M., Prasanta S., and Kashinath S. (2013). "Nonlinear vibration analysis of simply supported stiffened plate by a variational method." *Mechanics of Advanced Materials and Structures*, Vol. 20, No. 5, pp. 373-396, DOI: 10.1080/15376494.2011.627640.

Chen, C. S. (2007). "The nonlinear vibration of an initially stressed laminated plate." *Composites: Part B*, Vol. 38, No. 4, pp. 437-447, DOI: 10.1016/j.compositesb.2006.09.002.

Chen, C. S., Fung, C. P., and Chien, R. D. (2007). "Nonlinear vibration of an initially stressed laminated plate according to a higher-order theory." *Composite Structures*, Vol. 77, No. 4, pp. 521-532. DOI: 10.1016/j.compstruct.2005.08.004.

Chia, C. Y. (1980). *Non-linear analysis of plates*, McGraw-Hill, New York, NY, USA.

Dozio, L. and Ricciardi, M. (2009). "Free vibration analysis of ribbed plates by a combined analytical-numerical method." *Journal of Sound and Vibration*, Vol. 319, Nos. 1-2, pp. 681-697, DOI: 10.1016/j.jsv.2008.06.024.

Duc, N. D., Cong, P. H., Tuan, N. D., Tran, P., Anh, V. M., and Quang, V. D. (2016). "Nonlinear vibration and dynamic response of imperfect eccentrically stiffened shear deformable sandwich plate with functionally graded material in thermal environment." *Journal of Sandwich Structures & Materials,* Vol. 18, No. 4, pp. 445-473, DOI: 10.1177/1099636215602142.

Gabor, M. V. (2009). "Buckling and free vibration analysis of stiffened panels." *Thin-Walled Structures*, Vol. 47, No. 4, pp. 382-390, DOI: 10.1016/j.tws.2008.09.002.

Hassan, N. H. and El-Tawil, A. M. (2012). "A new technique of using homotopy analysis method for second order nonlinear differential equations." *Applied Mathematics and Computation*, Vol. 219, No. 2, pp. 708-728, DOI: 10.1016/j.amc.2012.06.065.

Hoseini, S. H., Pirbodaghi, T., Asghari, M., Farrahi G. H., and Ahmadian, M. T. (2008). "Nonlinear free vibration of conservative oscillators with inertia and static type cubic nonlinearities using homotopy analysis method." *Journal of Sound and Vibration*, Vol. 316, Nos. 1-5, pp. 263-273, DOI: 10.1016/j.jsv.2008.02.043.

Liao, S. J. (2003). *Beyond perturbation: Introduction to the homotopy analysis method,* CRC Press, Boca Raton, FL, USA.

Ma, N. J., Wang, R. H., and Han, Q. (2015). "Primary parametric resonance-primary resonance response of stiffened plates with moving boundary conditions." *Nonlinear Dynamics*, Vol. 79, No. 3, pp. 2207-2223, DOI: 10.1007/s11071-014-1806-2.

Ma, N. J., Wang, R. H., and Li, P. J. (2012). "Nonlinear dynamic response of a stiffened plate with four edges clamped under primary resonance excitation." *Nonlinear Dynamics*, Vol. 70, No. 1, pp. 627-648, DOI: 10.1007/s11071-012-0483-2.

Noseir, A. and Reddy, J. N. (1991). "A study of non-linear dynamic equations of higher-order deformation plate theories." *International Journal of Non-Linear Mechanics*, Vol. 26, No. 2, pp. 233-49, DOI: 10.1016/0020-7462(91)90054-w.

Peng, L. X., Liew, K. M., and Kitipornchai, S. (2006). "Buckling and free vibration analyses of stiffened plates using the FSDT mesh-free method." *Journal of Sound and Vibration*, Vol. 289, No. 3, pp. 421-449, DOI: 10.1016/j.jsv.2005.02.023.

Pirbodaghi, T., Ahmadian, M. T., and Fesanghary, M. (2009). "On the homotopy analysis method for non-linear vibration of beams."

Mechanics Research Communications, Vol. 36, No. 2, pp. 143-148, DOI: 10.1016/j.mechrescom.2008.08.001.

Sapountzakis, E. J. and Mokos, V. G. (2008). "An improved model for the dynamic analysis of plates stiffened by parallel beams." *Engineering Structures*, Vol. 30, No. 6, pp. 1720-1733, DOI: 10.1016/j.engstruct.2007.11.016.

Sheikh, A. H. and Mukhopadhyay, M. (2002). "Linear and nonlinear transient vibration analysis of stiffened plate structures." *Finite Elements in Analysis and Design*, Vol. 38, No. 6, pp. 477-502. DOI: 10.1016/s0168-874x(01)00081-6.

Xu, H. A., Du, J. T., and Li, W. L. (2010). "Vibrations of rectangular plates reinforced by any number of beams of arbitrary lengths and placement angles." *Journal of Sound and Vibration*, Vol. 329, No. 18, pp. 3759-3779, DOI: 10.1016/j.jsv.2010.03.023.

Yin, X. W., Wu, W. W., Li, H., and Zhong K. K. (2017). "Vibration transmission within beam-stiffened plate structures using dynamic stiffness method." *Procedia Engineering*, Vol. 199, pp. 411-416, DOI: 10.1016/j.proeng.2017.09.133.

Yuan, G. Q. and Jiang, W. K. (2017). "Vibration analysis of stiffened multi-plate structure based on a modified variational principle." *Journal of Vibration and Control*, Vol. 23, No. 17, pp. 2767-2781, DOI: 10.1177/1077546315621855.

Yuriy A. R. and Marina, V. S. (2006). "Dynamic stability of a circular pre-stressed elastic orthotropic plate subjected to shock excitation." *Shock and Vibration*, Vol. 13, No. 3, pp. 197-214, DOI: 10.1155/2006/142832.

Zheng, G. and Hu, Y. R. (2005). "Shake down effect of residual stress and its influence on the strength of rectangular plates in stiffened panels." *Journal of Ship Mechanics*, Vol. 9, No. 3, pp. 77-86. DOI: 1007-7294(2005)09-0077-10.

Appendix A.

$$g^1_{ijmn} = \rho h \int_0^a \int_0^b u^d_{ij} u^d_{mn} \mathrm{d}x\mathrm{d}y + \rho A_x \sum_{r=1}^{N_{sx}} \int_0^a u^d_{ij} u^d_{mn} \mathrm{d}x \Big|_{y=y_r} + \rho A_y \sum_{r=1}^{N_{sy}} \int_0^b u^d_{ij} u^d_{mn} \mathrm{d}y \Big|_{x=x_r} \tag{37}$$

$$c^1_{ij} = \sigma_{x0} h \int_0^a \int_0^b \frac{\partial u^d_{ij}}{\partial x} \mathrm{d}x\mathrm{d}y + \sigma_{sx0} A_x \sum_{r=1}^{N_{sx}} \int_0^a \frac{\partial u^d_{ij}}{\partial x} \mathrm{d}x \Big|_{y=y_r} \tag{38}$$

$$d^1_{ijmn} = \frac{Eh}{1-\mu^2} \int_0^a \int_0^b \frac{\partial u^d_{ij}}{\partial x} \frac{\partial u^d_{mn}}{\partial x} \mathrm{d}x\mathrm{d}y + \frac{Eh}{1+\mu} \int_0^a \int_0^b \frac{\partial u^d_{ij}}{\partial y} \frac{\partial u^d_{mn}}{\partial y} \mathrm{d}x\mathrm{d}y + EA_x \sum_{r=1}^{N_{sx}} \int_0^a \frac{\partial u^d_{ij}}{\partial x} \frac{\partial u^d_{mn}}{\partial x} \mathrm{d}x \Big|_{y=y_r} \tag{39}$$

$$d^2_{ijmn} = \frac{\mu Eh}{1-\mu^2} \int_0^a \int_0^b \frac{\partial u^d_{ij}}{\partial x} \frac{\partial v^d_{mn}}{\partial y} \mathrm{d}x\mathrm{d}y + \frac{Eh}{1+\mu} \int_0^a \int_0^b \frac{\partial u^d_{ij}}{\partial y} \frac{\partial v^d_{mn}}{\partial x} \mathrm{d}x\mathrm{d}y \tag{40}$$

$$d^3_{ijmn} = \frac{-E}{1-\mu^2} \int_{\Omega_p} z \frac{\partial u^d_{ij}}{\partial x} \frac{\partial^2 w^d_{mn}}{\partial x^2} \mathrm{d}V + \frac{-\mu E}{1-\mu^2} \int_{\Omega_p} z \frac{\partial u^d_{ij}}{\partial x} \frac{\partial^2 w^d_{mn}}{\partial y^2} \mathrm{d}V + \frac{2E}{1+\mu} \int_{\Omega_p} z \frac{\partial u^d_{ij}}{\partial y} \frac{\partial^2 w^d_{mn}}{\partial x \partial y} \mathrm{d}V - E \int_{\Omega_{sx}} z \frac{\partial u^d_{ij}}{\partial x} \frac{\partial^2 w^d_{mn}}{\partial x^2} \mathrm{d}V \tag{41}$$

$$e^1_{ijmnkl} = \frac{Eh}{2\left(1-\mu^2\right)} \int_0^a \int_0^b \frac{\partial u^d_{ij}}{\partial x} \frac{\partial w^d_{mn}}{\partial x} \frac{\partial w^d_{kl}}{\partial x} \mathrm{d}x\mathrm{d}y + \frac{\mu Eh}{2\left(1-\mu^2\right)} \int_0^a \int_0^b \frac{\partial u^d_{ij}}{\partial x} \frac{\partial w^d_{mn}}{\partial y} \frac{\partial w^d_{kl}}{\partial y} \mathrm{d}x\mathrm{d}y \quad \frac{Eh}{1+\mu} \int_0^a \int_0^b \frac{\partial u^d_{ij}}{\partial y} \frac{\partial w^d_{mn}}{\partial x} \frac{\partial w^d_{kl}}{\partial y} \mathrm{d}x\mathrm{d}y + \frac{EA_x}{2} \sum_{r=1}^{N_{sx}} \int_0^a \frac{\partial u^d_{ij}}{\partial x} \frac{\partial w^d_{mn}}{\partial x} \frac{\partial w^d_{kl}}{\partial y} \mathrm{d}x \Big|_{y=y_r} \tag{42}$$

$$g^2_{ijmn} = \rho h \int_0^a \int_0^b v^d_{ij} v^d_{mn} \mathrm{d}x\mathrm{d}y + \rho A_x \sum_{r=1}^{N_{sx}} \int_0^a v^d_{ij} v^d_{mn} \mathrm{d}x \Big|_{y=y_r} + \rho A_y \sum_{r=1}^{N_{sy}} \int_0^b v^d_{ij} v^d_{mn} \mathrm{d}y \Big|_{x=x_r} \tag{43}$$

$$c^2_{ij} = \sigma_{y0} h \int_0^a \int_0^b \frac{\partial v^d_{ij}}{\partial y} \mathrm{d}x\mathrm{d}y + \sigma_{sy0} A_y \sum_{r=1}^{N_{sy}} \int_0^b \frac{\partial v^d_{ij}}{\partial y} \mathrm{d}x \Big|_{x=x_r} \tag{44}$$

$$d^4_{ijmn} = \frac{\mu Eh}{1-\mu^2} \int_0^a \int_0^b \frac{\partial v^d_{ij}}{\partial y} \frac{\partial u^d_{mn}}{\partial x} \mathrm{d}x\mathrm{d}y \quad + \frac{Eh}{1+\mu} \int_0^a \int_0^b \frac{\partial v^d_{ij}}{\partial x} \frac{\partial u^d_{mn}}{\partial y} \mathrm{d}x\mathrm{d}y \tag{45}$$

$$d^5_{ijmn} = \frac{Eh}{1-\mu^2} \int_0^a \int_0^b \frac{\partial v^d_{ij}}{\partial y} \frac{\partial v^d_{mn}}{\partial y} \mathrm{d}x\mathrm{d}y + \frac{Eh}{1+\mu} \int_0^a \int_0^b \frac{\partial v^d_{ij}}{\partial x} \frac{\partial v^d_{mn}}{\partial x} \mathrm{d}x\mathrm{d}y + EA_y \sum_{r=1}^{N_{sy}} \int_0^b \frac{\partial v^d_{ij}}{\partial y} \frac{\partial v^d_{mn}}{\partial y} \mathrm{d}y \Big|_{x=x_r} \tag{46}$$

$$d^6_{ijmn} = \frac{-E}{1-\mu^2} \int_{\Omega_p} z \frac{\partial v^d_{ij}}{\partial y} \frac{\partial^2 w^d_{mn}}{\partial x^2} \mathrm{d}V + \frac{-\mu E}{1-\mu^2} \int_{\Omega_p} z \frac{\partial v^d_{ij}}{\partial y} \frac{\partial^2 w^d_{mn}}{\partial y^2} \mathrm{d}V + \frac{2E}{1+\mu} \int_{\Omega_p} z \frac{\partial v^d_{ij}}{\partial x} \frac{\partial^2 w^d_{mn}}{\partial x \partial y} \mathrm{d}V - E \int_{\Omega_{sy}} z \frac{\partial v^d_{ij}}{\partial y} \frac{\partial^2 w^d_{mn}}{\partial x^2} \mathrm{d}V \tag{47}$$

$$e^2_{ijmnkl} = \frac{Eh}{2\left(1-\mu^2\right)} \int_0^a \int_0^b \frac{\partial v^d_{ij}}{\partial y} \frac{\partial w^d_{mn}}{\partial x} \frac{\partial w^d_{kl}}{\partial x} \mathrm{d}x\mathrm{d}y + \frac{\mu Eh}{2\left(1-\mu^2\right)} \int_0^a \int_0^b \frac{\partial v^d_{ij}}{\partial y} \frac{\partial w^d_{mn}}{\partial y} \frac{\partial w^d_{kl}}{\partial y} \mathrm{d}x\mathrm{d}y \quad \frac{Eh}{1+\mu} \int_0^a \int_0^b \frac{\partial v^d_{ij}}{\partial x} \frac{\partial w^d_{mn}}{\partial x} \frac{\partial w^d_{kl}}{\partial y} \mathrm{d}x\mathrm{d}y + \frac{EA_y}{2} \sum_{r=1}^{N_{sy}} \int_0^b \frac{\partial v^d_{ij}}{\partial y} \frac{\partial w^d_{mn}}{\partial x} \frac{\partial w^d_{kl}}{\partial y} \mathrm{d}y \Big|_{x=x_r} \tag{48}$$

$$g^3_{ijmn} = \rho h \int_0^a \int_0^b w^d_{ij} w^d_{mn} \mathrm{d}x\mathrm{d}y + \rho A_x \sum_{r=1}^{N_{sx}} \int_0^a w^d_{ij} w^d_{mn} \mathrm{d}x \Big|_{y=y_r} + \rho A_y \sum_{r=1}^{N_{sy}} \int_0^b w^d_{ij} w^d_{mn} \mathrm{d}y \Big|_{x=x_r} \tag{49}$$

$$c^3_{ij} = -\sigma_{x0} \int_{\Omega_p} z \frac{\partial^2 w^d_{ij}}{\partial x^2} \mathrm{d}V - \sigma_{y0} \int_{\Omega_p} z \frac{\partial^2 w^d_{ij}}{\partial y^2} \mathrm{d}V - E \sum_{r=1}^{N_{sx}} \int_{\Omega_{sx}} z \frac{\partial^2 w^d_{ij}}{\partial x^2} \mathrm{d}V \Big|_{y=y_r} - E \sum_{r=1}^{N_{sy}} \int_{\Omega_{sy}} z \frac{\partial^2 w^d_{ij}}{\partial y^2} \mathrm{d}V \Big|_{x=x_r} \tag{50}$$

$$d^7_{ijmn} = \frac{-E}{1-\mu^2} \int_{\Omega_p} z \frac{\partial w^d_{ij}}{\partial x^2} \frac{\partial^2 u^d_{mn}}{\partial x} \mathrm{d}V + \frac{-\mu E}{1-\mu^2} \int_{\Omega_p} z \frac{\partial^2 w^d_{ij}}{\partial y^2} \frac{\partial u^d_{mn}}{\partial x} \mathrm{d}V + \frac{2E}{1+\mu} \int_{\Omega_p} z \frac{\partial^2 w^d_{ij}}{\partial x \partial y} \frac{\partial u^d_{mn}}{\partial y} \mathrm{d}V - E \int_{\Omega_{sx}} z \frac{\partial^2 w^d_{ij}}{\partial x^2} \frac{\partial u^d_{mn}}{\partial x} \mathrm{d}V \tag{51}$$

$$d_{ijmn}^{8}=\frac{-E}{1-\mu^{2}}\int_{\Omega_p} z\frac{\partial^{2}w_{ij}^{d}}{\partial x^{2}}\frac{\partial v_{mn}^{d}}{\partial y}\mathrm{d}V+\frac{-\mu E}{1-\mu^{2}}\int_{\Omega_p} z\frac{\partial^{2}w_{ij}^{d}}{\partial y^{2}}\frac{\partial v_{mn}^{d}}{\partial y}\mathrm{d}V$$
$$+\frac{2E}{1+\mu}\int_{\Omega_p} z\frac{\partial^{2}w_{ij}^{d}}{\partial x\partial y}\frac{\partial v_{mn}^{d}}{\partial x}\mathrm{d}V-E\int_{\Omega_{sy}} z\frac{\partial^{2}w_{ij}^{d}}{\partial x^{2}}\frac{\partial v_{mn}^{d}}{\partial y}\mathrm{d}V \tag{52}$$

$$d_{ijmn}^{9}=\sigma_{x0}h\int_{0}^{a}\int_{0}^{b}\frac{\partial w_{ij}^{d}}{\partial x}\frac{\partial w_{mn}^{d}}{\partial x}\mathrm{d}x\mathrm{d}y+\sigma_{y0}h\int_{0}^{a}\int_{0}^{b}\frac{\partial w_{ij}^{d}}{\partial y}\frac{\partial w_{mn}^{d}}{\partial y}\mathrm{d}x\mathrm{d}y$$
$$+\frac{E}{1-\mu^{2}}\int_{\Omega_p} z^{2}\frac{\partial^{2}w_{ij}^{d}}{\partial x^{2}}\frac{\partial^{2}w_{mn}^{d}}{\partial x^{2}}\mathrm{d}V+\frac{E}{1-\mu^{2}}\int_{\Omega_p} z^{2}\frac{\partial^{2}w_{ij}^{d}}{\partial y^{2}}\frac{\partial^{2}w_{mn}^{d}}{\partial y^{2}}\mathrm{d}V$$
$$+\frac{2\mu E}{1-\mu^{2}}\int_{\Omega_p} z^{2}\frac{\partial^{2}w_{ij}^{d}}{\partial x^{2}}\frac{\partial^{2}w_{mn}^{d}}{\partial y^{2}}\mathrm{d}V+\frac{4E}{1+\mu}\int_{\Omega_p} z^{2}\frac{\partial^{2}w_{ij}^{d}}{\partial x\partial y}\frac{\partial^{2}w_{mn}^{d}}{\partial x\partial y}\mathrm{d}V$$
$$+\sigma_{xx0}A_x\sum_{r=1}^{N_{sx}}\int_{0}^{b}\frac{\partial w_{ij}^{d}}{\partial x}\frac{\partial w_{mn}^{d}}{\partial x}\mathrm{d}x\Big|_{y=y_r}+E\int_{\Omega_{sx}} z^{2}\frac{\partial^{2}w_{ij}^{d}}{\partial x^{2}}\frac{\partial^{2}w_{mn}^{d}}{\partial x^{2}}\mathrm{d}V$$
$$+\sigma_{sy0}A_y\sum_{r=1}^{N_{sy}}\int_{0}^{b}\frac{\partial w_{ij}^{d}}{\partial y}\frac{\partial w_{mn}^{d}}{\partial y}\mathrm{d}y\Big|_{x=x_r}+E\int_{\Omega_{sy}} z^{2}\frac{\partial^{2}w_{ij}^{d}}{\partial y^{2}}\frac{\partial^{2}w_{mn}^{d}}{\partial y^{2}}\mathrm{d}V \tag{53}$$

$$e_{ijmnkl}^{3}=\frac{Eh}{1-\mu^{2}}\int_{0}^{a}\int_{0}^{b}\frac{\partial w_{ij}^{d}}{\partial x}\frac{\partial u_{mn}^{d}}{\partial x}\frac{\partial w_{kl}^{d}}{\partial x}\mathrm{d}x\mathrm{d}y$$
$$+\frac{\mu Eh}{1-\mu^{2}}\int_{0}^{a}\int_{0}^{b}\frac{\partial w_{ij}^{d}}{\partial y}\frac{\partial u_{mn}^{d}}{\partial x}\frac{\partial w_{kl}^{d}}{\partial y}\mathrm{d}x\mathrm{d}y \tag{54}$$

$$e_{ijmnkl}^{4}=\frac{Eh}{1-\mu^{2}}\int_{0}^{a}\int_{0}^{b}\frac{\partial w_{ij}^{d}}{\partial x}\frac{\partial v_{mn}^{d}}{\partial y}\frac{\partial w_{kl}^{d}}{\partial x}\mathrm{d}x\mathrm{d}y$$
$$+\frac{\mu Eh}{1-\mu^{2}}\int_{0}^{a}\int_{0}^{b}\frac{\partial w_{ij}^{d}}{\partial y}\frac{\partial v_{mn}^{d}}{\partial y}\frac{\partial w_{kl}^{d}}{\partial y}\mathrm{d}x\mathrm{d}y\ \ \frac{2Eh}{1+\mu}\int_{0}^{a}\int_{0}^{b}\frac{\partial w_{ij}^{d}}{\partial x}\frac{\partial v_{mn}^{d}}{\partial x}\frac{\partial w_{kl}^{d}}{\partial y}\mathrm{d}x\mathrm{d}y$$
$$+EA_y\sum_{r=1}^{N_{sy}}\int_{0}^{b}\frac{\partial w_{ij}^{d}}{\partial x}\frac{\partial v_{mn}^{d}}{\partial y}\frac{\partial w_{kl}^{d}}{\partial y}\mathrm{d}y\Big|_{x=x_r} \tag{55}$$

$$e_{ijmnkl}^{5}=\frac{-3E}{2\left(1-\mu^{2}\right)}\int_{\Omega_p} z\frac{\partial w_{ij}^{d}}{\partial x}\frac{\partial w_{mn}^{d}}{\partial x}\frac{\partial^{2}w_{kl}^{d}}{\partial x^{2}}\mathrm{d}V$$
$$+\frac{-3E}{2\left(1-\mu^{2}\right)}\int_{\Omega_p} z\frac{\partial w_{ij}^{d}}{\partial y}\frac{\partial w_{mn}^{d}}{\partial y}\frac{\partial^{2}w_{kl}^{d}}{\partial y^{2}}\mathrm{d}V$$
$$+\frac{-3\mu E}{2\left(1-\mu^{2}\right)}\int_{\Omega_p} z\frac{\partial w_{ij}^{d}}{\partial x}\frac{\partial w_{mn}^{d}}{\partial x}\frac{\partial^{2}w_{kl}^{d}}{\partial y^{2}}\mathrm{d}V$$
$$+\frac{-3\mu E}{2\left(1-\mu^{2}\right)}\int_{\Omega_p} z\frac{\partial w_{ij}^{d}}{\partial y}\frac{\partial w_{mn}^{d}}{\partial y}\frac{\partial^{2}w_{kl}^{d}}{\partial x^{2}}\mathrm{d}V\ +\frac{6E}{1+\mu}\int_{\Omega_p} z\frac{\partial w_{ij}^{d}}{\partial x}\frac{\partial w_{mn}^{d}}{\partial y}\frac{\partial^{2}w_{kl}^{d}}{\partial x\partial y}\mathrm{d}V$$

$$+\frac{-3E}{2}\sum_{r=1}^{N_{sx}}\int_{\Omega_{sx}} z\frac{\partial w_{ij}^{d}}{\partial x}\frac{\partial w_{mn}^{d}}{\partial x}\frac{\partial^{2}w_{kl}^{d}}{\partial x^{2}}\mathrm{d}V$$
$$+\frac{-3E}{2}\sum_{r=1}^{N_{sy}}\int_{\Omega_{sy}} z\frac{\partial w_{ij}^{d}}{\partial y}\frac{\partial w_{mn}^{d}}{\partial y}\frac{\partial^{2}w_{kl}^{d}}{\partial y^{2}}\mathrm{d}V \tag{56}$$

$$f_{ijmnklpq}=\frac{Eh}{2\left(1-\mu^{2}\right)}\int_{0}^{a}\int_{0}^{b}\frac{\partial w_{ij}^{d}}{\partial x}\frac{\partial w_{mn}^{d}}{\partial x}\frac{\partial w_{kl}^{d}}{\partial x}\frac{\partial w_{pq}^{d}}{\partial x}\mathrm{d}x\mathrm{d}y$$
$$+\frac{Eh}{2\left(1-\mu^{2}\right)}\int_{0}^{a}\int_{0}^{b}\frac{\partial w_{ij}^{d}}{\partial y}\frac{\partial w_{mn}^{d}}{\partial y}\frac{\partial w_{kl}^{d}}{\partial y}\frac{\partial w_{pq}^{d}}{\partial y}\mathrm{d}x\mathrm{d}y$$
$$+\frac{\mu Eh}{1-\mu^{2}}\int_{0}^{a}\int_{0}^{b}\frac{\partial w_{ij}^{d}}{\partial x}\frac{\partial w_{mn}^{d}}{\partial x}\frac{\partial w_{kl}^{d}}{\partial y}\frac{\partial w_{pq}^{d}}{\partial y}\mathrm{d}x\mathrm{d}y$$
$$+\frac{2Eh}{1+\mu}\int_{0}^{a}\int_{0}^{b}\frac{\partial w_{ij}^{d}}{\partial x}\frac{\partial w_{mn}^{d}}{\partial x}\frac{\partial w_{kl}^{d}}{\partial y}\frac{\partial w_{pq}^{d}}{\partial y}\mathrm{d}x\mathrm{d}y$$
$$+\frac{EA_x}{2}\sum_{r=1}^{N_{sx}}\int_{0}^{a}\frac{\partial w_{ij}^{d}}{\partial x}\frac{\partial w_{mn}^{d}}{\partial x}\frac{\partial w_{kl}^{d}}{\partial x}\frac{\partial w_{pq}^{d}}{\partial x}\mathrm{d}x\Big|_{y=y_r}$$
$$+\frac{EA_y}{2}\sum_{r=1}^{N_{sy}}\int_{0}^{b}\frac{\partial w_{ij}^{d}}{\partial y}\frac{\partial v_{mn}^{d}}{\partial y}\frac{\partial w_{kl}^{d}}{\partial y}\frac{\partial w_{pq}^{d}}{\partial y}\mathrm{d}y\Big|_{x=x_r} \tag{57}$$